Analysis of mechanical and microstructural properties of high performance concretes containing nanosilica and silica fume

Jéssica Zamboni Schiavon[1], Pietra Moraes Borges[1],
Sérgio Roberto da Silva[1], Jairo José de Oliveira Andrade[1]

[1] Programa de Pós-Graduação em Engenharia e Tecnologia de Materiais, PGETEMA/PUCRS, Av. Ipiranga, 6681, Prédio 30, Parternon, Porto Alegre, RS, Brasil.
e-mails: jessica.squiavon@acad.pucrs.br, pietra.borges@acad.pucrs.br, sergio.roberto@acad.pucrs.br, jairo.andrade@pucrs.br

ABSTRACT

The use of nanomaterials in concrete has shown promise, and the use of several types in cementitious compounds has been found to guarantee greater physical–mechanical properties and improvements in microstructure. The use of mineral admixtures, such as silica fume, ensures the improvement of the interfacial transition zone (ITZ) between aggregate and paste in high-performance concrete (HPC). Thus, this work evaluates the performance of superplasticizer additive with colloidal nanosilica suspension and slurried silica fume with HPC and its macro- and micro-structural properties. The mechanical (i.e., compressive strength and elastic modulus) and microstructural properties via (scanning electron microscopy and X-ray micro tomography) of concretes with 1.5 and 3% nanosilica and 5 and 10% silica fume included in the evaluation methods in this study. The results indicate that, with the use of mineral admixtures, the compressive strength and elastic modulus of concrete increased significantly. The concrete with the use of 10% silica fume and 3% nanosilica resulted in a showed an increased strength over 75% at 28 days. Besides that, for same w/b = 0.35 the elastic modulus increased by 36% compared with the reference concrete. The microstructural investigations show that the nanosilica and silica fume led to a densification of microstructure, which is responsible for the improvement of HPC performance.

Keywords: high performance concrete, silica fume, nanosilica, mechanical properties, microstructure.

1. INTRODUCTION

Concrete represents one of the most widely used construction materials worldwide by volume. Efforts are needed to design and develop more ecologically friendly concrete with improved performance in strength and durability [1]. The high-performance concrete (HPC) has become vital for the construction of skyscrapers from a structural and economical point of view. Higher mechanical strength is crucial to carry loads and reduce the cross-sections of vertical load-bearing elements (columns and walls), while a high modulus of elasticity is necessary to limit deflections and wind sway [2]. Thus, HPC has become a much stronger competitor for super tall buildings, compared to structural steel. The super-tall buildings in the future will be made of HPC, with a steel or composite spire at the top [2]. High-performance concrete consists of a mixture with supplementary materials, superplasticizer admixture and a low ratio water/binder. These materials make the cast-in-place of concrete easier by reducing the amount of transverse reinforcement, improving performance, attenuating damage in critical regions, minimizing residual deformations and reducing repair costs in structures located in seismic areas [3].

The potential of using pozzolanic materials has been explored, through the use of slag, palm oil ash, fly ash, silica fume, metakaolin and rice husk ash [4]. The supplementary cementitious materials (SCMs) used by the cement industry are limestone and industrial by-products, such as fly ash from coal plants, blast furnace slag from pig iron production and silica fume from the Ferro-silicon industry. In addition, natural pozzolans and thermally activated clay minerals (for example, metakaolin) are used, which, together with industrial by-products, characterized by high levels of silica or silica and alumina [5]. Fly ash and metakaolin demonstrated efficiency in this regard, with the filling of smaller pores of the concrete reported due to the increase in pozzolanic reactions [6]. The combined use of SCMs in concrete contributes to an increase in the generation of CSH gel and consequently the densification of the microstructure. The presence of SCMs in concrete provides greater production of C-S-H and, consequently, improves the physical-mechanical properties, which

is important for the improvement of high-performance concrete (HPC) [7-9]. The use of fly ash, for example, the compressive strength ranges from 45 to 67 MPa, favoring its contribution to structural concrete [10]. As a by-product of the manufacture of silicon and ferrosilicon alloys, silica fume contains more than 90% SiO_2 and is present in spherical shape with average diameters about 100 times smaller than cement particles. The high specific surface area of silica fume is 10 to 20 times greater than that of other pozzolanic materials [1]. Silica fume is advantageous for use in concrete, mainly due to its high specific surface and the amount of amorphous silica, which increases the formation of hydrated products at an early age [9]. The addition of silica fume influences the thickness of the transition zone of the concrete cement paste, and the degree of orientation of the CH crystals, therefore, the mechanical properties and durability are improved [11]. ANWAR and EMARAH [12] demonstrated that the use of silica fume could decrease the carbonation of cement paste products and increase resistance to attack by chlorides, improving their durability, due to the pozzolanic effects.

In the same way, the addition of silica fume improved the microstructure of all the specimens, irrespective of the aggregate (granite and quartzite) types in concrete [13]. The increase in strength can be observed in the replacement of cement by silica fume up to 20%, and from 10 to 15% of silica fume provides the optimum result. In addition, the resistance increases with increasing aging ages compared to the reference mixture. The incorporation of silica by up to 25% provides an improvement in the durability properties of concrete while being affected if the silica fume content exceeds 25% [14]. The high specific surface of silica fume makes it difficult to handle the material, in addition to worsening the workability of cementitious materials, unless it is made in the form of paste. Despite this, fine particles fill the spaces between the cement paste, thus producing a denser paste, decreasing the permeability and porosity of the composite [15].

The application of nanotechnology in cement-based materials is still under research. The results of experimental tests of concrete samples with nanomaterials have demonstrated that they can increase the compressive strength and durability of concretes [16]. The nano (nm) size of the nanoparticles produces a filling effect of cement pastes compared to materials on a micro (μ) scale [7]. The most favorable nanoparticles for use in cementitious materials are nano (SiO_2, Al_2O_3, Fe_2O_3, TiO_2, although there are studies containing nano (ZrO_2 and ZnO_2). However, nanomaterials such as nanosilica, carbon nanotube and graphene oxide, have been used as nano-reinforcement to improve its properties (compressive strength, microstructure and durability) together with supplementary cementitious materials such as fly ash [17]. According to SAID *et al*. [18] nanosilica can be found as a colloidal suspension and compacted dry grains. The incorporation of nanosilica in cement solutions is more effective, depending on the adequate dispersion of particles in the concrete mass, which reduces agglomeration and is preferable for practical purposes [18].

XU, WANG and ZUO [19] investigated the relationship between the macro and microscale properties of concretes with the addition of 1% nanosilica. Their results showed an increase in compressive strength and elastic modulus after 3 days. According to NAZERIGIVI and NAJIGIVI [20] the cement paste could be benefited with nanosilica nanoparticles up to a maximum level of 2.0% and with particles of 15 nm; and another 1.5% with particles with 80 nm. LI and GAO [21] reported that the ideal nanosilica content in concrete is 1%, while NILI and EHSANI [22] found that the addition of 5% nanosilica increased the compressive strength of concrete, and densified the microstructure of the concrete. According to WANG *et al.* [23] the mechanical properties of cement pastes were improved with the addition of 3% nano-SiO_2, the compressive strength at three days increased by 33.2% and at 28 days it increased by 18.5%.

However, the difficulty of dispersing nanomaterials adversely affects the performance of cementitious materials and remains unresolved. FENG *et al.* [24] used polycarboxylate superplasticizer and nano-SiO_2 particles for use in cementitious materials. From a content greater than 0.5%, the nanosilica sample and the reference sample have very similar volume fractions of gel pores and medium capillary pores. This factor was explained by the possible agglomeration of the nanosilica and by the compact gel; structure of the hydration products, the diffusion of dehydrates is blocked and, therefore, produces a more porous structure [24]. The microstructure of mixtures containing nanosilica is characterized by phases containing calcium hydroxide, etringite, AFm and C-S-H, identified [25].

High-performance concrete is very important nowadays, as there are several benefits associated (high compressive strength, besides being useful for environments that need concrete with great durability). However, the design of the compound and the combined use of mineral additions with chemical additives are not yet fully understood [10]. Due to the relevance of high-performance concrete, which is significant for constructions that require extremely efficient structural materials, this work seeks to use a mineral addition combined with a nanomaterial. This study demonstrates the efficiency of silica fume in suspension, as well as the polycarboxylate superplasticizer with nanosilica in order to evaluate the efficiency of materials in mechanical properties (compressive strength and elastic modulus), porosity via x-ray micro tomography and the effect of

densification microstructure via scanning electron microscopy. Thus, this investigation contributes to the understanding of the effect of nanosilica and silica fume on the macro and microscale properties of high-performance concrete considering the synergistic benefit.

2. MATERIALS AND EXPERIMENTAL PROCEDURES

2.1 Materials

Brazilian high early strength Portland cement, similar to ASTM Type C 150 III [26], was used in concrete mixtures, presenting a specific surface, density, and compressive strength at 28 days equal to 1425 cm²/g, 3.05 g/cm3, and 51.3 MPa, respectively. Silica fume was used composed of silica dispersed in an aqueous solution, containing a solids content of 50% and 50% water. This water amount from silica fume needs to be discounted later from the water of the mixtures made. Slurried silica fume presents a BET surface area equal to 18.42 m²/g, a spherical shape and an average particle size of 0.3 µm. In Table 1, its properties are presented according to the manufacturer. In Fig. 1 is presented the morphology of silica fume particles and their main elements obtained by EDS analysis.

Table 1: Properties of silica fume.

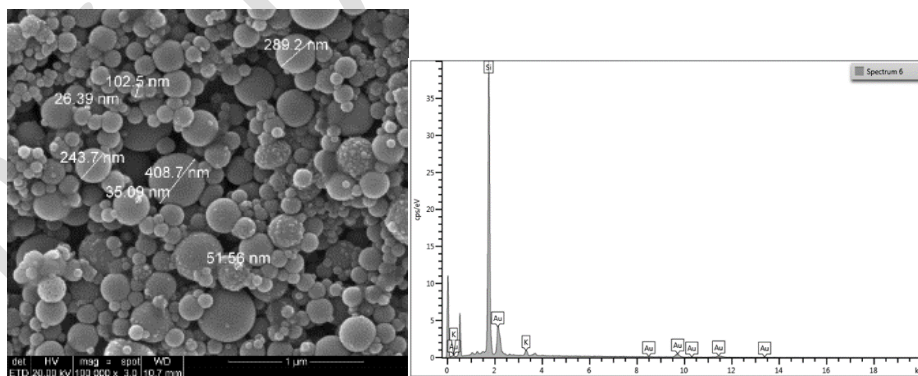| PROPERTY	RESULT
Appearance	Dark gray liquid
SiO_2, %	94.5
Loss of ignition, %	2.2
Alkaline equivalent Na_2O, %	0.2
Solid content, %	49
Sieve 45 µm (325 Mesh), %	0.2
Bulk density, (g/cm³)	1.38
Viscosity, (s)	7.1
pH	7.1

Figure 1: SEM image (a) and EDS spectrum (b) of silica fume particles.

The other product is a polycarboxylate based superplasticizer additive and is industrially incorporated in to colloidal nanosilica suspension. This stabilized nanosilica has BET surface area characterization equal to 250 m²/g, an average particle size of 13 nm and bulk density 1.06 g/cm³. For concretes that did not contain stabilized nanosilica, a polycarboxylate-based superplasticizer content bulk density 1.1 g/cm³ was used to maintain adequate workability. The fine aggregate used was river sand, and the coarse aggregate was of basaltic origin. Their characteristics are presented in Table 2.

Table 2: Characteristics of the aggregates.

TEST	FINE AGGREGATE	BRAZILIAN STANDARD	COARSE AGGREGATE	BRAZILIAN STANDARD
Apparent specific gravity (g/cm²)	2.60	NBR NM 52 [27]	2.92	NBR NM 52 [27]
Bulk density (g/cm³)	1.50	NBR NM 45 [28]	1.54	NBR NM 45 [28]
Fineness modulus	2.56	NBR NM 248 [29]	7.01	NBR NM 248 [29]
Maximum size (mm)	4.75		19	

2.2 Experimental Procedures

Several proportioned mixes were designed to evaluate the effects of silica fume and nanosilica in three concrete classes, depending on their water/binder (w/b) ratio: 0.25 (HPC 1), 0.30 (HPC 2), and 0.35 (HPC 3). Two levels of nanosilica (1.5 and 3%) were used in concretes, similar to those used in previous studies whose levels were 2.0% [30, 31]. The silica fume were used with two levels (5 and 10%). According to MEHTA and ASHISH [14] the silica fume improves the hydration of the cement paste, but as the percentage of silica substitution grows, the workability of the concrete mixture decreases due to the increase in the surface area of the silica. The increase in resistance can be observed in the use of silica fume by up to 20%. Considering the production of all combinations, a complete experiment would ordinarily be necessary for all 27-mix proportions. Before the execution of each mixture, a manual homogenization was carried out to disperse the silica in the aqueous suspension. To optimize the amount of concrete mixtures, a fractional factorial project was used, given that only some of the total amount of tests would be performed. Many researchers have used fractional factorial design [32, 33]. The mix-proportioning method proposed by AÏTCIN [34], specifically developed for high-performance concretes, was used. The mix design used is presented in Table 3, Due the large number of mixtures and each of them uses a different parameter, in order to identify the behavior of each material (nanosilica and silica fume) isolated mixtures were performed. The workability was varied due to the other factors were fixed in the mixtures such as w/b ratio and additive content.

Table 3: Characteristics of the aggregates.

Mix design	w/b	SF (%)	NS (%)	CONTENT (kg/m³)					SP (%)	SLUMP (mm)
				CEMENT	SILICA FUME	NANO-SILICA	FINE AGGREGATE	COARSE AGGREGATE		
HPC1-SF0-NS0	0.25	0	0	520	0	0	874	989	2	225
HPC1-SF10-NS0	0.25	10	0	468	52	0	821	989	2	170
HPC1-SF5-NS1.5	0.25	5	1.5	494	26	7	854	989	0	180
HPC1-SF0-NS3	0.25	0	3	520	0	16	876	989	0	205
HPC1-SF10-NS3	0.25	10	3	468	52	14	822	989	0	210
HPC2-SF5-NS0	0.3	5	0	412	22	0	926	989	2	140
HPC2-SF0-NS1.5	0.3	0	1.5	433	0	7	954	989	0	195
HPC2-SF5-NS1.5	0.3	5	1.5	412	22	6.26	931	989	0	150
HPC2-SF10-NS1.5	0.3	10	1.5	390	43	5.84	909	989	0	200
HPC2-SF5-NS3	0.3	5	3	412	22	12	927	989	0	215
HPC3-SF0-NS0	0.35	0	0	371	0	0	1001	989	2	150

HPC3-SF10-NS0	0.35	10	0	334	37	0	963	989	2	160
HPC3-SF5-NS1.5	0.35	5	1.5	353	19	5	987	989	0	190
HPC3-SF0-NS3	0.35	0	3	371	0	11	1003	989	0	175
HPC3-SF10-NS3	0.35	10	3	334	37	10	964	989	0	220

The concretes casting was defined as NBR 5738 [35] using cylindrical specimens (10×15 cm) for each mix design. After 24 hrs. the specimens were demolded and submerged in water until they reached their ages for the mechanical tests. The ages were defined at 7 and 28 days for the compressive-strength tests (three samples for each mix proportion by age), following the criteria of NBR 5739 [36] and NBR 8522 [37], respectively. To evaluate the microstructure of the concretes at 28 days, samples of the central part of the test specimen were analyzed. For the Scanning Electron Microscopy (SEM) with Energy Dispersive X-Ray Spectroscopy (EDS) the equipment was used (Inspect F50 – FEI), operating voltage 0.3 to 30 kV and point resolution of 1.2 nm. The concrete samples were broken into small fragments, and sample size 0.5 x 0.5 cm, identified, and dried in an oven. The porosity images were captured by the microtomograph (SkyScan 1173–Bruker), operating voltage of 50 kV, and electric current of 0.3 mA, resolution of 10 μm and sample size 1.0 x 1.0 cm. The reconstructed images edited by data viewer software, in which a sample size of 5×5×5 pixels was adopted for the region of interest. CT-Vox and CT-Vol software were used to generate 3D models, and CTan software was used to calculate the porosity.

3. RESULTS AND DISCUSSION

3.1 Compressive strength (fc) and elastic modulus (Ec)

Analysis of variance (ANOVA) was used to verify if the nanosilica and silica fume content presented a statistically significant effect on the properties investigated, in which a confidence level of 95% was adopted for all analysis performed. A non-linear estimation model was developed for the compressive strength and elastic modulus from the obtained experimental data. Equations 1 and 2, respectively present the models for fc and Ec, developed through the experimental data.

$$f_c = -1018.47 + 208.68 \times Age - 338.22 \times \frac{w}{b} + 4.07 \times NS - 6.44 \times SF + 26.95 \times \frac{w}{b} \times SF - 5.94 \times Age^2 - 0.76 \times NS^2, \tag{1}$$

$$R^2 = 0.89,$$

$$Ec = 65.4556 - 64.8823 \times \frac{w}{b} + e^{\left(0.4494 \times \frac{w}{b} \times SF\right)} + 11.3464 \times \frac{w}{b} \times NS, \tag{2}$$

$$R^2 = 0.88.$$

Parameter f_c = compressive strength (MPa); E_c = elastic modulus (GPa); NS = nanosilica (%); SF = silica fume (%); Age = age of samples; and w/b = water/binder ratio.

The R² determined for each model was greater than or equal to 0.88, meaning that the model could explain at least 88% of variability in the properties investigated. In Table 4, the ANOVA results for the models are presented.

Table 4: ANOVA for the models.

RESPONSE	SOURCE	SUM OF SQUARES	DEGREES OF FREEDOM	MEAN SQUARE	F-TEST	P-VALUE
f_c	Model	112612.1	8.0	14076.51	327.5529	0.000000
	Residual	687.6	16.0	42.97		
	Total	113299.7	24.0			
E_c	Regression	33879.76	5.0	6775.952	4511.956	0.000000
	Residual	10.51	7.0	1.502		
	Total	33890.27	12.0			

Considering the model presented in Equation 1, Figure 2 represents the effect of silica fume on the compressive strength of concretes with 3% nanosilica at 7 and 28 days for all w/b ratios investigated. The line represents the model behavior (Equation 1), and the points are the average experimental values with their standard deviation.
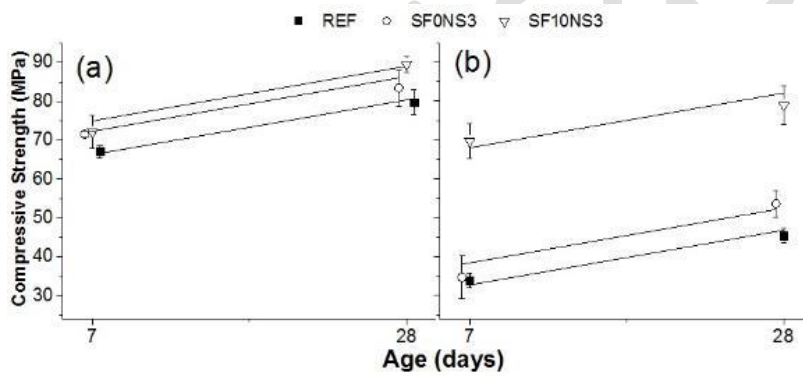
Figure 2: Effect of silica fume on the compressive strength of concretes with 3% nanosilica: (a) w/b = 0.25 and (b) w/b = 0.35.

Figure 3 presents the effect of nanosilica incorporation on the compressive strength of concretes with 10% silica fume for w/b = 0.25 and 0.35.
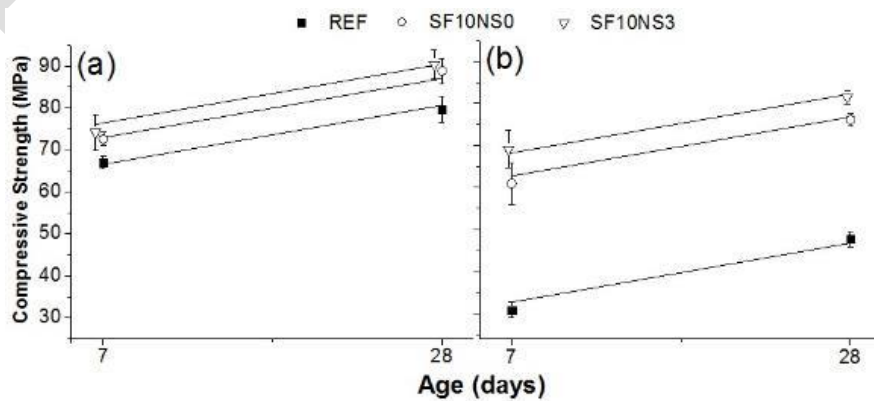
Figure 3: Effect of nanosilica on the compressive strength of concretes with 10% silica fume: (a) w/b = 0.25 and (b) w/b = 0.35.

An increase in the compressive strength was observed with the addition of silica fume and nanosilica in concrete, as shown in Figure 4. Compared with the reference concrete, the HPC3-SF10-NS3 showed an increased strength of 75.6% at 28 days. The concrete using only 10% silica fume (HPC3-SF10-NS0) exhibited a strength value equal to 76.75 MPa, 60% higher than reference concrete (46.79 MPa) at 28 days. These results presented similar tendencies to those obtained by ELAHI *et al*. [38], which found a 102% increase in the compressive strength of concrete using 7.5% silica fume at the same age. According to OLIVEIRA *et al*. [39] in high performance concrete the amount of silica fume present is responsible for strengthening the interfacial transition zone at the paste/aggregate, contributing to the increase in compressive strength, where the authors obtained a result of (64 and 73.4 MPa) at 28 days.

The HPC2-SF0-NS3 concrete showed an increase in compressive strength of only 8.5% when compared to the reference concrete (HPC2-SF0-NS0). When producing a high-performance concrete and when the content of nanosilica was higher, there was a higher generation of C-S-H because of its higher reactivity, allowing the hydration products to grow on their surfaces, forming a more dense C-S-H gel. However, because the addition of nanosilica can significantly increase the viscosity of the cement mixtures, a large amount of air can be trapped in the concrete, which can increase the porosity of the material [40]. According to FRAGA *et al*. [41] a method could be used to disperse these particles as ultrasonication and special mixers. From the ultrasonication there is a greater production of C-S-H, refinement of the pores and greater compressive strength from this process, improving the effectiveness of these materials with the dis-persion of these particles.

Figure 3 shows this behavior in the HPC, although the high reactivity of the nanosilica particles increased the initial strength of the concrete, when the content of nanosilica was high, the effect did not appear as significant [22]. With the reduction in the w/b ratio to 0.25, the additives together did not present a significant effect. The use of 10% silica fume and 3% nanosilica resulted in a 10.5% increase in compressive strength at 28 days, compared with the reference concrete. From the results of compressive strength, it can be stated that the ideal content for the use of stabilized nanosilica is near 1.5% in concrete, optimizing the properties and providing material savings in concrete structures.

The behavior of the elastic modulus in concrete with 3% nanosilica and the addition of different amounts of silica fume can be observed in Fig. 4, whereas in Fig. 5, the effect of the addition of nanosilica on the elastic modulus of concrete with 10% silica fume is presented.
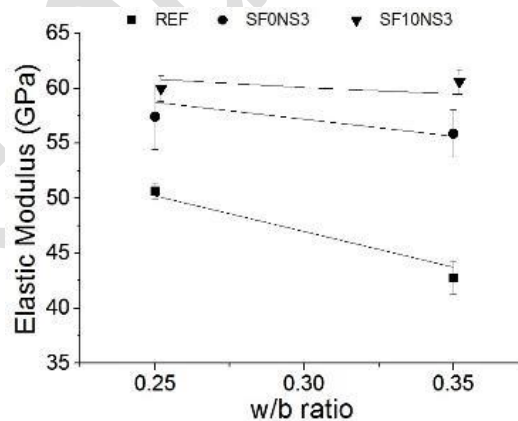

Figure 4: Effect of silica fume on the elastic modulus (Ec) of concrete with 3% nanosilica.
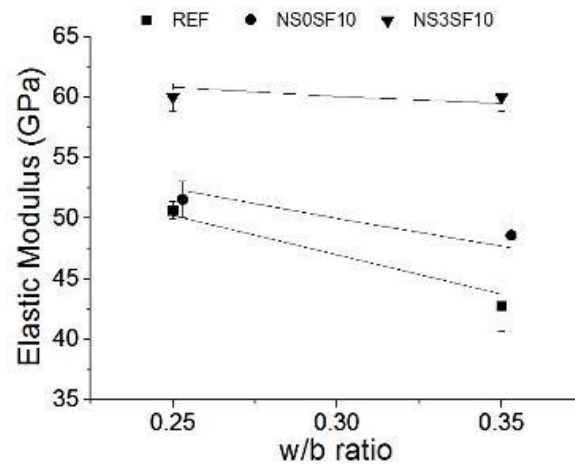
Figure 5: Effect of nanosilica on the elastic modulus (Ec) of concrete with 10% of silica fume.

The elastic modulus at 28 days increased as w/b was reduced from 0.35 to 0.25. With the addition of 10% silica fume and 3% of nanosilica, the elastic modulus increased by 21.1% compared with the reference concrete at w/b = 0.25. Meanwhile, for w/b = 0.30 and 0.35, the increases were 27.9% and 36%, respectively. Piasta *et al*. [42] found that the elastic modulus of the high-performance concrete with w/b = 0.28 was 47.1 GPa, whereas the elastic modulus of the concrete with 1% nanosilica showed an increase of 13%, attributed to the effects of nanosilica modification on the microstructure [19]. Because the trend of the results of both fc and Ec were consistent, that is, as the silica fume and nanosilica content were incorporated into the concretes, an improvement in the properties occurred.

3.2 SEM with EDS and X-ray microtomography

SEM with energy dispersive X-ray spectroscopy (EDS) analysis was used to verify the microstructure of concretes investigated and to provide a better understanding of results. The ITZ of the reference concrete Figure 1(a) presented a microstructure with C-S-H predominance and high porosity and voids. According to the EDS results presented in Figure 6(b), a large amount of Ca and small peaks of C, O, and Si can be observed.
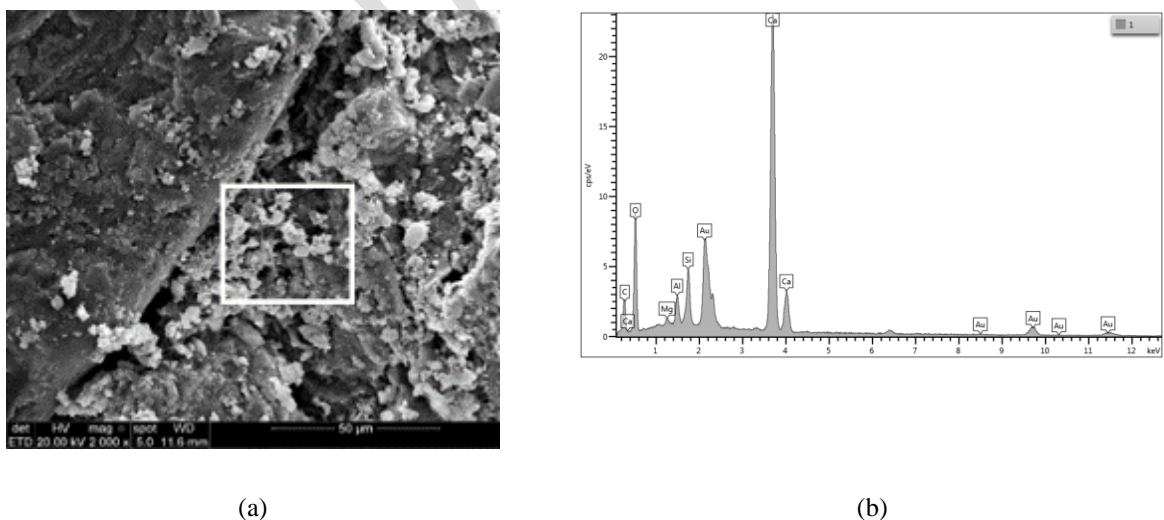

(a)

(b)

Figure 6: SEM for concrete (a) HPC3-SF0-NS0, (b) EDS of highlight area.

Figure 7(a) reveals that the concrete paste contained possible C-S-H with dense structure with the presence of gel pores between the C-S-H layers. These results are similar to those found by JI [43], JO *et al.* [44], YU *et al.* [40], and DU *et al.* [45], who demonstrated the performance of nanosilica in the refinement of cement paste. Analyzing the EDS of Figure 7(b), the presence of calcium-dominated element peaks and

smaller amounts of Si, Ca, and O were observed. According to JALAL *et al.* [31] the significant increase in compressive strength with silica fume and nanosilica was caused by the rapid consumption of CH produced during Portland-cement hydration, especially in the early ages, related to the high reactivity of particles. Therefore, the hydration of the cement was accelerated, and larger volumes of hydrated products were formed.
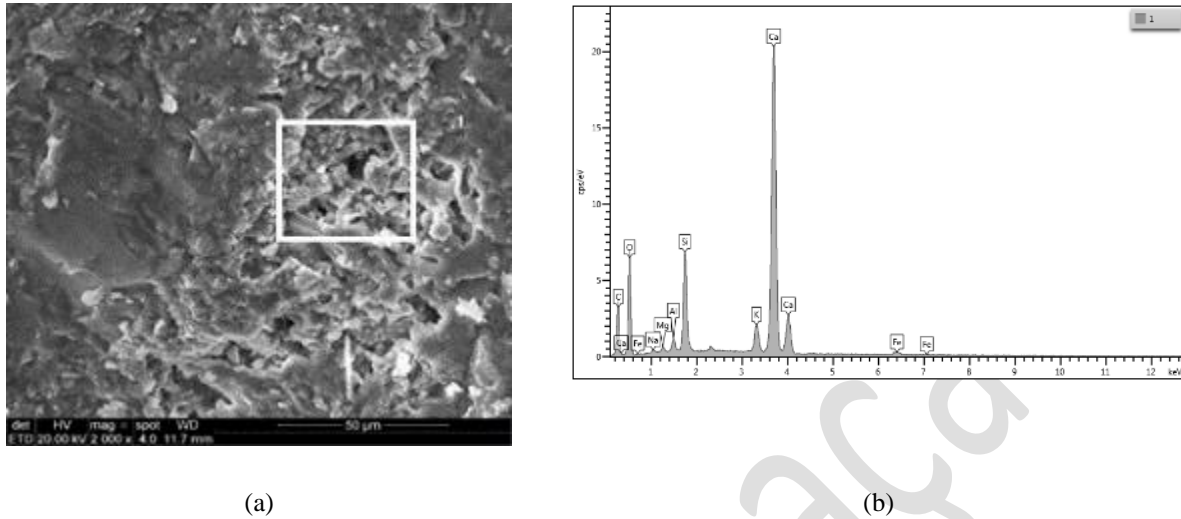

(a)   (b)

Figure 7: SEM for (a) concrete HPC3-SF10-NS3; (b) EDS of highlight area.

Figures 8(a) and 8(b) show the 3% stabilized nanosilica concrete with a magnification of 5,000× and 20,000×, respectively. A predominance of CH crystals, ettringite, and more porous cementitious pastes are observed with pores in the regions around CH and ettringite. The images confirm the results of the compressive strength, because the nanosilica for this content did not present an increase in resistance as high as the silica fume used in an isolated manner. According to KHALOO *et al.* [30], the nanosilica particles presented a high specific surface area, which could result in a greater possibility of forming agglomerates of nanoparticles, affecting the efficiency of nanosilica, particularly thinner and more reactive grains.
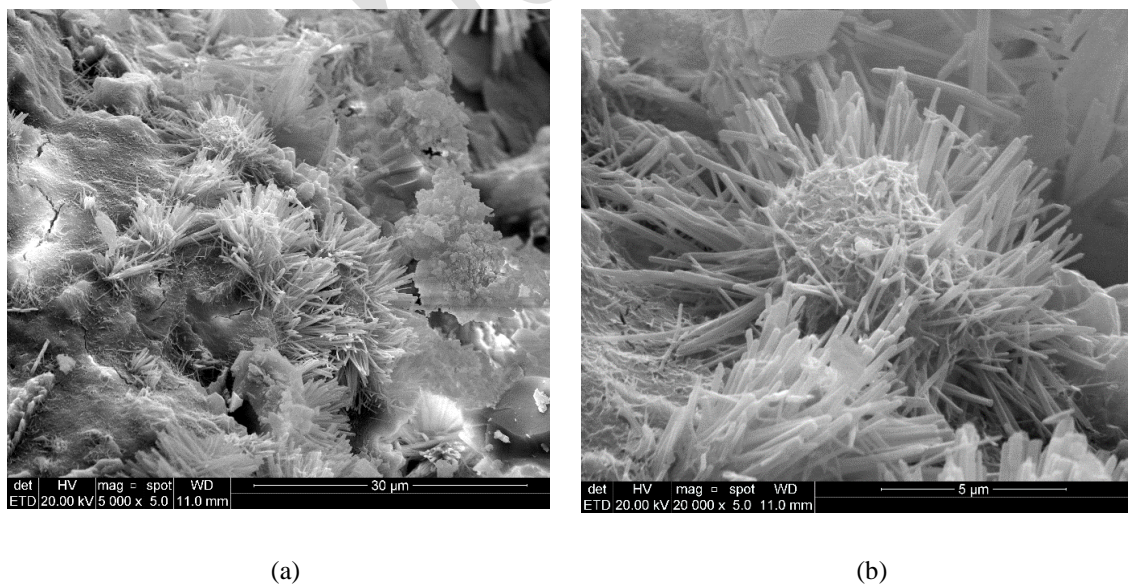

(a)   (b)

Figure 8: SEM for concrete with w/b = 0.35 and 3% nanosilica: (a) magnification 5,000×, (b) magnification 20,000×.

Figure 9(a) shows the presence of a predominantly C-S-H region, because the predominant Si peaks and, in smaller amounts, Al, O, and Ca peaks (Fig. 9b) are characteristic of exclusively nanosilica concretes.

However, the microstructure of concrete with silica fume presented a similar morphology (Figure 10a). Figure 10b shows the presence of silicon peaks and lower proportions of O and Ca. The presence of the Al peak must be related to the presence of aluminosilicate compound.
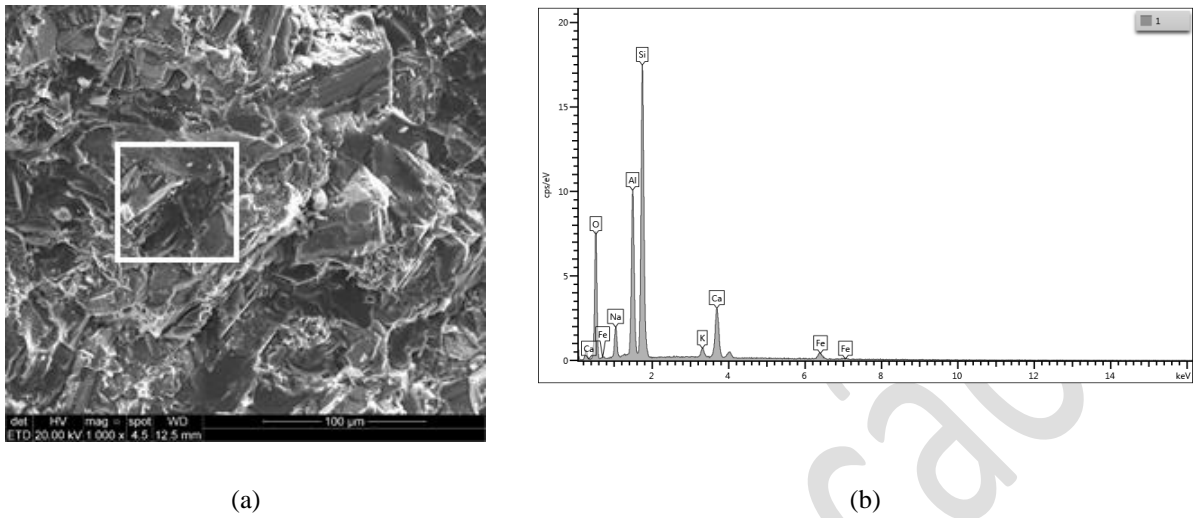

(a)   (b)

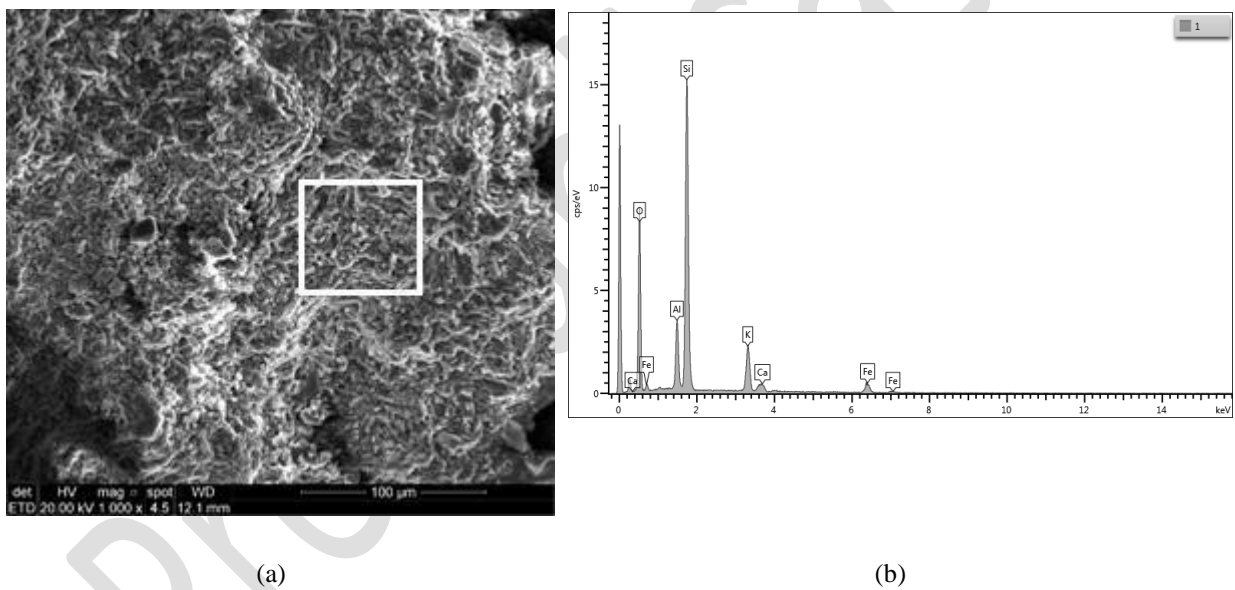**Figure 9:** SEM for (a) concrete HPC1-SF0-NS3, (b) EDS of highlight area.

(a)   (b)

Figure 10: SEM for (a) concrete HPC1-SF10-NS0, (b) EDS of highlight area.

Generally, it can be inferred that the variable influencing concrete densification the most is the w/b ratio, followed by the number of mineral admixtures. There is a direct correlation between the results obtained through macro-structural analysis and the microstructural investigations. In the case of w/b = 0.35, for example, as the silica fume content increased, there was an increase in the compressive strength of the concretes. However, SEM analysis showed the predominance of C-S-H with dense structure. Because of its fineness and high content of amorphous silicon dioxide, silica fume is a very reactive pozzolanic material, which, upon reaction, decreases and modifies the orientation of CH crystals [46]. Additionally, silica-fume particles filled the spaces between the grains of cement, resulting in a more homogeneous cementitious matrix and transition zone. Figures 11, 12, 13 show the reconstructed images and porosities obtained from X-ray microtomography, indicating that the light-gray region corresponds to the large aggregate, whereas the dark gray portion corresponds to the cementitious paste. The circular points represent the pores. The images were reconstructed in cubic samples of 5×5×5 pixels. The heterogeneous microstructure of the material and the phases (i.e., aggregates, paste, and pores) are clearly perceived, and the results of the figures are similar to

those obtained by Chung *et al*. [47], where the authors showed the distribution of the voids and the constituents of the concrete.
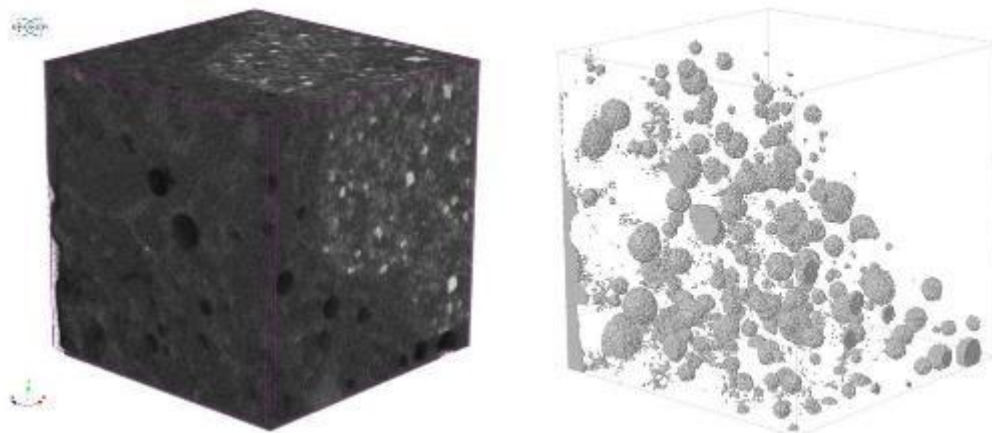

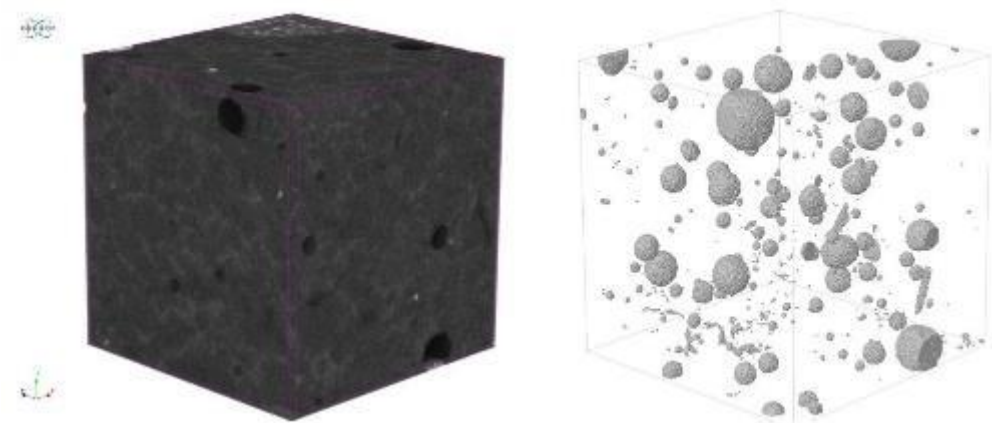**Figure 11:** Reconstructed image and pores of reference concrete with w/b = 0.35.

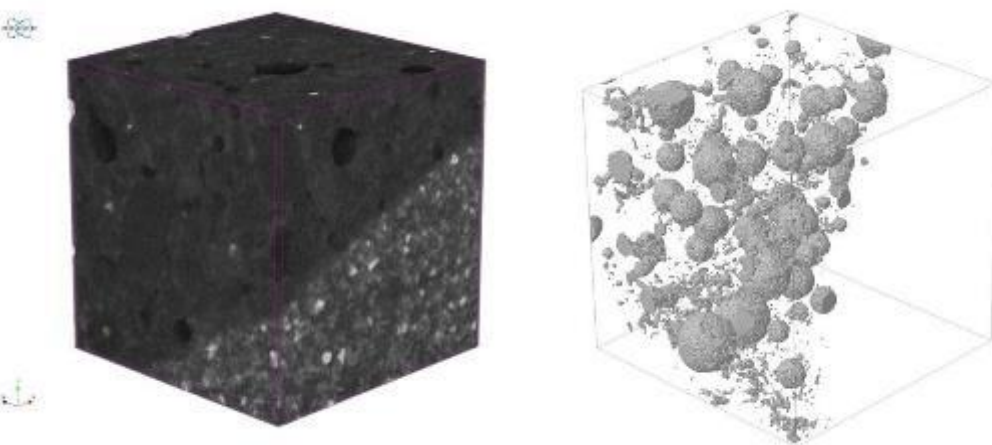**Figure 12:** Reconstructed image and concrete pores with 10% silica fume and w/b = 0.35.

Figure 13: Reconstructed image and pores of concrete with 3% nanosilica and w/b = 0.35

The percentage of white pixels, in relation to the total pixels of the image, yields the porosity calculation. All

pores are considered open and closed according to the selected volume of interest. The results, shown in Fig. 14, show that the reference concrete at 3.99% exhibited the highest porosity. From the three analyses, the sample with silica fume exhibited the lowest porosity, 3.27%, whereas nanosilica had a porosity of 3.78%. These values were similar to those found by Lu *et al*. [48], who found a decrease in porosity values of 6.2% for the reference concrete and 6% for the concrete with 7% silica fume.
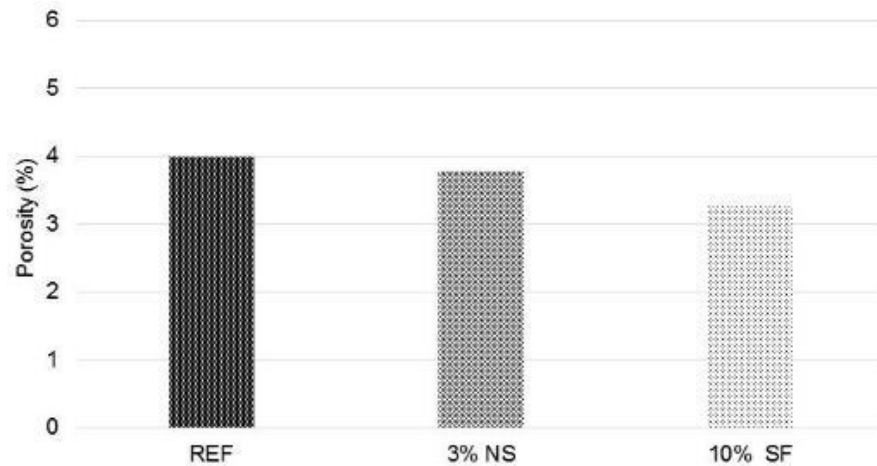

Figure 14: Total porosity of samples (%) obtained by X-ray microtomography for concretes with w/b = 0.35.

Using X-ray micro tomography, it was verified that it is possible to obtain images showing the porosity of the concretes. However, the samples need to be smaller to increase the resolution of the images, as reported by Leite and Monteiro [49]. Additionally, the values obtained by the CTan software reiterate the results of the mechanical tests, in which the use of silica fume promotes the reduction of porosity. The silica particles react with the CH, forming additional phases, such as low- and high-density C-S-H. Unreacted silica particles act as filler, reducing the porosity of the concrete matrix [50]. According to the compressive strength (fc) and elastic modulus (Ec) results, silica fume provided a significant difference when compared to nanosilica in concrete porosity. However, according to Feng *et al*. [24] comparing the reference sample and the nanosilica sample both have very similar volume fractions of gel pores and medium capillary pores. This factor was explained by the possible agglomeration of nanosilica and the compact gel structure of hydration products, the diffusion of unhydrates is blocked and thus produces a more porous structure.

4. CONCLUSIONS

The high-performance concretes composed some combinations such superplasticizer additive with colloidal nanosilica suspension and slurried silica fume in was studied in this work. The focus on materials and test procedures per-formed in this investigation demonstrated that:

High-performance concrete containing silica fume exhibited higher compressive strength and elastic modulus results than mixtures using only stabilized nanosilica for all investigated w/b.

The results of concrete using only 10% silica fume and w/b 0.35 showed an increased strength of 47% (76.75 MPa) than stabilized nanosilica concrete (at 52.19 MPa) age 28 days. The elastic modulus HPC3-SF10-NS3 increased by 36% compared with the reference concrete.

According to the microstructure investigation, the concretes with the simultaneous combination nanosilica and silica fume presented a dense and uniform microstructure, with a predominance of C-S-H particles, related to the synergistic effect.

The HPC containing only polycarboxylate superplasticizer with nano-SiO_2 presents of CH crystals, ettringite, and more pores in the regions around CH and ettringite. The x-ray micro tomography images showed a porosity similar to high-performance concrete without nanosilica.

The silica fume and nanosilica incorporation in any levels promotes an increase in the hydration of the paste, increasing the amount of additional CSH. Based on the results, verified an increase of microstructural densification of cement matrix, with the minimization of interfacial transition zone.

5. ACKNOWLEDGMENTS

6. BIBLIOGRAFHY

[1] NICOARA, A.I., STOICA, A.E., VRABEC, M., *et al.* "End-of-Life Materials Used as Supplementary Cementitious Materials in the Concrete Industry", *Materials*, v.13, n.8, 2020.

[2] NEHDI, M.L. "Only tall things cast shadows: Opportunities, challenges and research needs of self-consolidating concrete in super-tall buildings", *Construction and Building Materials,* v. 48, p. 80–90, 2013.

[3] PEREIRO-BARCELÓ, J., BONET, J.L., GÓMEZ-PORTILLO, S., *et al.* "Ductility of high-performance concrete and very-high-performance concrete elements with Ni-Ti reinforcements", *Construction and Building Materials*, v.175, p. 531–551, 2018.

[4] HEMALATHA, M.S., SANTHANAM, M. "Characterizing supplementary cementing materials in blended mortars", *Construction and Building Materials*, v. 191, p. 440–459, 2018.

[5] SKIBSTED, J., SNELLINGS, R. "Reactivity of supplementary cementitious materials (SCMs) in cement blends", *Cement and Concrete Research*, v. 124, n. 105799, 2019.

[6] LU, D., TANG, Z., ZHANG, L., *et al.* "Effects of Combined Usage of Supplementary Cementitious Materials on the Thermal Properties and Microstructure of High-Performance Concrete at High Temperatures", *Materials*, v. 13, n. 8, 2020.

[7] NORHASRI, M.S.M., HAMIDAH, M.S., FADZIL, A.M. "Applications of using nano material in concrete: A review", *Construction and Building Materials*, v. 133, p. 91–97, 2017.

[8] LOTHENBACH, B., SCRIVENER, K., HOOTON, R. D. "Supplementary cementitious materials", *Cement and Concrete Research,* v. 41, p. 1244–1256, 2011.

[9] MAZLOOM, M., RAMEZANIANPOUR, A.A., BROOKS, J.J. "Effect of silica fume on mechanical properties of high-strength concrete", *Cement and Concrete Composites*, v. 26, p. 347–357, 2004.

[10] VÁZQUEZ-RODRÍGUEZ, F.J., ELIZONDO-VILLAREAL, N., VERÁSTEGUI, L.H., *et al.* "Effect of Mineral Aggregates and Chemical Admixtures as Internal Curing Agents on the Mechanical Properties and Durability of High-Performance Concrete", *Materials*, v. 13, n.9, 2020.

[11] SIDDIQUE, R., CHAHAL, N. "Use of silicon and ferrosilicon industry by-products (silica fume) in cement paste and mortar", *Resources, Conservation & Recycling*, p. 739–744, 2011.

[12] ANWAR, M., EMARAH, D.A. "Resistance of concrete containing ternary cementitious blends to chloride attack and carbonation", *Journal of Materials Research and Technology*, 2020.

[13] CHUNG, S.Y., KIM, J., LEHMANN, C., *et al.* "Investigation of phase composition and microstructure of foamed cement paste with different supplementary cementing materials", *Cement and Concrete Composites*. v. 109, n.103560, 2020.

[14] MEHTA, A., ASHISH, D. K. "Silica fume and waste glass in cement concrete production: A review", *Journal of Building Engineering*, v. 29, n.100888, 2020.

[15] TAYLOR, H.F.W., Cement Chemistry, 2nd ed., London, Thomas Telford, 1997.

[16] BAUTISTA-GUTIERREZ, K.P., HERRERA-MAY, A.L., SANTAMARÍA-LÓPEZ, J.M., *et al.* "Recent Progress in Nanomaterials for Modern Concrete Infrastructure: Advantages and Challenges", *Materials*, v. 12, n.21, 2019.

[17] XU, G., SHI, X. "Characteristics and applications of fly ash as a sustainable construction material: A state-of-the-art review", *Resources, Conservation & Recycling*, v. 136, p. 95–109, 2018.

[18] SAID, A.M., ZEIDAN, M.S., BASSUONI, M.T., *et al.* "Properties of concrete incorporating nano-silica", *Construction and Building Materials*, v. 36, p. 838–844, 2012.

[19] XU, J., WANG, B., ZUO, J. "Modification effects of nanosilica on the interfacial transition zone in con-

crete: A multiscale approach", *Cement and Concrete Composites*, v.81, p. 1-10, 2017.

[20] NAZERIGIVI, A., NAJIGIVI, A. "Study on mechanical properties of ternary blended concrete containing two different sizes of nano-SiO$_2$", *Composites Part B: Engineering*, v. 167, p. 20–24, 2019.

[21] LI, G., GAO, B. "Effect of level SiO$_2$ and level CaCO$_3$ on concrete performance", *Journal of Railway Engineering Society*, v. 28, p. 131–136, 2006.

[22] NILI, M., EHSANI, A. "Investigating the effect of the cement paste and transition zone on strength development of concrete containing nanosilica and silica fume", *Materials & Design*, v. 75, p. 174–83, 2015.

[23] WANG, L., ZHENG, D., ZHANG, S., *et al.* "Effect of Nano-SiO$_2$ on the Hydration and Microstructure of Portland cement", *Nanomaterials*, v.6, n.12, 2016.

[24] FENG, P., CHANG, H., LIU, X., *et al.* "The significance of dispersion of nano-SiO$_2$ on early age hydration of cement pastes", *Materials & Design*, v. 186, 2020.

[25] SUN, D., WU, K., SHI, H., *et al.* "Effect of interfacial transition zone on the transport of sulfate ions in concrete", *Construction and Building Materials*, v. 192, p. 28–37, 2018.

[26] AMERICAN SOCIETY FOR TESTING AND MATERIALS. ASTM. Standard Specification for Portland cement. West Conshohocken, PA: American Society for Testing and Materials, 2004.

[27] ASSOCIAÇÃO BRASILEIRA DE NORMAS TÉCNICAS. NBR NM 52. Fine aggregate - Determination of specific gravity and apparent specific mass, Rio de Janeiro, 2009.

[28] ASSOCIAÇÃO BRASILEIRA DE NORMAS TÉCNICAS. NBR NM 45. Aggregates - Determination of the unit weight and air-void contents, Rio de Janeiro, 2006.

[29] ASSOCIAÇÃO BRASILEIRA DE NORMAS TÉCNICAS. NBR NM 248. Aggregates - Sieve analysis of fine and coarse aggregates, Rio de Janeiro, 2003.

[30] KHALOO, A., MOBINI, M.H., HOSSEINI, P. "Influence of different types of nano-SiO$_2$ particles on properties of high-performance concrete", *Construction and Building Materials*, v.113, p. 188–201, 2016.

[31] JALAL, M., POULADKHAN, A., HARANDI, O.F., *et al.* "Comparative study on effects of Class F fly ash, nano silica and silica fume on properties of high performance self-compacting concrete", *Construction and Building Materials*, v. 94, p. 90–104, 2015.

[32] SILVA, S.R., ANDRADE, J.J.O. "Investigation of mechanical properties and carbonation of concretes with construction and demolition waste and fly ash", Construction and Building Materials, v. 153, p. 704–15, 2017.

[33] CABRAL, A.E.B., SCHALCH, V., MOLIN, D.C.C.D., *et al.* "Mechanical properties modeling of recycled aggregate concrete", *Construction and Building Materials*, v. 24, p. 421–30, 2010.

[34] AÏTCIN, P.C., Concreto de Alto Desempenho, São Paulo, PINI, 2000.

[35] ASSOCIAÇÃO BRASILEIRA DE NORMAS TÉCNICAS. NBR 5738. Procedure for molding and curing concrete test specimens, Rio de Janeiro, 2016.

[36] ASSOCIAÇÃO BRASILEIRA DE NORMAS TÉCNICAS. NBR 5739. Concrete - Compression test of cylindrical specimens, Rio de Janeiro, 2018.

[37] ASSOCIAÇÃO BRASILEIRA DE NORMAS TÉCNICAS. NBR 8522. Concrete - Determination of static modulus of elasticity and deformation by compression, Rio de Janeiro, 2017.

[38] ELAHI, A., BASHEER, P.A.M, NANUKUTTAN, S.V., *et al.* "Mechanical and durability properties of high performance concretes containing supplementary cementitious materials", *Construction and Building Materials*, v. 24, n. 3, p. 292-299, 2010.

[39] OLIVEIRA, C.O., MACIEL, G.D.F., DE CASTRO, A.L., *et al.* "Impacto do conceito de empacotamento de partículas na dosagem de concretos de alto desempenho", *Matéria (Rio J.) [online]*, v. 23, n. 1, 11962, 2018.

[40] YU, R., TANG, P., SPIESZ, P., *et al.* "A study of multiple effects of nano-silica and hybrid fibres on the properties of Ultra-High Performance Fibre Reinforced Concrete (UHPFRC) incorporating waste bottom ash (WBA)", *Construction and Building Materials*, v. 60, p. 98–110, 2014.

[41] FRAGA, Y.S.B., REGO, J.H.S., CAPUZZO, V.M.S., *et al.* "Efeito da ultrasonicação da sílica ativa e da nanossílica coloidal em pastas de cimento", *Matéria (Rio J.) [online]*, v. 25, n.4, 12847, 2020.

[42] PIASTA, W., GÓRA, J., BUDZYŃSKI, W. "Stress-strain relationships and modulus of elasticity of rocks and of ordinary and high performance concretes", *Construction and Building Materials*, v. 153, p. 728–739, 2017.

[43] JI, T. "Preliminary study on the water permeability and microstructure of concrete incorporating nano-SiO_2*", Cement and Concrete Research*, v. 35, p. 1943–1947, 2005.

[44] JO, B.W., KIM, C.H., TAE, G.H., *et al.* "Characteristics of cement mortar with nano-SiO2 particles", *Construction and Building Materials*. v. 21, p. 1351–1355, 2007.

[45] DU, H., DU, S., LIU, X. "Durability performances of concrete with nano-silica", *Construction and Building Materials*, v.73, p. 705-712, 2014.

[46] KHAN, M.I, SIDDIQUE, R. "Utilization of silica fume in concrete: Review of durability properties", *Resources, Conservation & Recycling,* v. 57, p. 30–35, 2011.

[47] CHUNG, S.Y., ELRAHMAN, M.A., Stephan, D. "Investigation of the effects of anisotropic pores on material properties of insulating concrete using computed tomography and probabilistic methods", *Energy and Buildings*, v.125, p. 122–129, 2016.

[48] LU, S., LANDIS, E.N., KEANE, D.T. "X-ray microtomographic studies of pore structure and permeability in Portland cement concrete", *Materials and Structures*, v. 39, p. 611–620, 2006.

[49] LEITE, M.B., MONTEIRO, P.J.M. "Microstructural analysis of recycled concrete using X-ray micro tomography", *Cement and Concrete Research*, v. 81, p. 38–48, 2016.

[50] MADDALENA, R., HAMILTON, A. "Low-pressure silica injection for porosity reduction in cementitious materials", *Construction and Building Materials*, v. 134, p. 610–616, 2017.

ORCID
Jéssica Zamboni Schiavon   https://orcid.org/0000-0001-9156-2794
Pietra Moraes Borges   https://orcid.org/0000-0003-3152-6569
Sérgio Roberto da Silva   https://orcid.org/0000-0002-9843-002X
Jairo José de Oliveira Andrade   https://orcid.org/0000-0003-2073-6763